catalysts

MDPI

Article

Mining, Identification, and Characterization of Three Xylanases from the Microbiota of *T. fuciformis* with Its Companion Strains

Yanhuan Lin [1], Changle Li [2], Chenxin Wei [2], Hui Lin [3,*] and Liaoyuan Zhang [2,*]

[1] College of Food Engineering, Zhangzhou Institute of Technology, Zhangzhou 363000, China; linyanhuan@fjzzit.edu.cn
[2] College of Life Sciences, Fujian Agriculture and Forestry University, Fuzhou 350002, China; 3215411004@stu.fafu.edu.cn (C.W.)
[3] Institute of Edible Fungi, Fujian Academy of Agricultural Sciences, Fuzhou 350012, China
* Correspondence: 2170517002@fafu.edu.cn (H.L.); 000q121064@fafu.edu.cn (L.Z.); Tel.: +86-591-83789492 (H.L. & L.Z.); Fax: +86-591-83789121 (L.Z.)

Abstract: Microbial xylanase has wide application in bioenergy, animal feed, environmental protection, the pulp and paper industry, and agricultural development. In this study, three xylanases from the microbiota of *T. fuciformis* with its companion strains were identified by metagenomics sequencing. The three enzymes were subjected to cloning and expression in *E. coli* or *P. pastoris*, purification, and characterization for their properties. The results showed that *As*Xyn1, from *Annulohypoxylon stygium*, among the three enzymes possessed high thermostability at 40 °C and broad pH tolerance in the range of 2.0–10.0, exhibiting its application potential. Furthermore, it was found that post-translational modification (such as glycosylation) of *As*Xyn1 enzyme modulated its activity, kinetic parameters, and thermostability. These results and findings provided a hint for enzyme modification and design in future.

Keywords: xylanase; *T. fuciformis*; companion strain; metagenome; heterologous expression

Citation: Lin, Y.; Li, C.; Wei, C.; Lin, H.; Zhang, L. Mining, Identification, and Characterization of Three Xylanases from the Microbiota of *T. fuciformis* with Its Companion Strains. *Catalysts* **2024**, *14*, 15. https://doi.org/10.3390/catal14010015

Academic Editor: Jose M. Guisan

Received: 20 November 2023
Revised: 19 December 2023
Accepted: 19 December 2023
Published: 24 December 2023

1. Introduction

Lignocellulosic biomass is the most abundant polysaccharide-containing renewable resource on earth, and mainly consists of a mixture of various complex carbohydrates, namely cellulose, hemicellulose, and lignin [1]. Xylan, as a typical hemicellulose composition, constitutes about one-third of the total dry weight in lignocellulosic biomass [2]. It is a heteroglycan constituted by β-1,4-linked xylose residues with side branches of α-glucuronic acid and α-arabinofuranose. In order to complete the conversion of xylan, an array of carbohydrate-active enzymes (CAZymes) is required, called xylanolytic enzymes [3]. These enzymes are mostly extracellular, are produced mainly by various microorganisms, including bacteria and fungi, which act in a concerted fashion to degrade xylan into its individual monosaccharide components. Of these, xylanase (endo-1,4-β-xylanase, EC 3.2.1.8) is one of the crucial biocatalysts to cleave the β-1,4-glycosidic bonds of the xylan backbone to produce xylooligosaccharides of different lengths [4].

Microbial xylanase has been widely applied in bioenergy, animal feed, environmental protection, the pulp and paper industry, and agricultural development [5]. Therefore, xylanase production with a higher yield and activity at a low cost is desired and required. In this respect, the isolation and identification of new genes encoding xylanases from some novel microbial sources represent alternative methods. Xylanases are widespread in nature, and have been reported in many microorganisms. Among microbial sources, filamentous fungi are relevant in that they secrete extracellular xylanases at higher levels than those observed in yeasts and bacteria. *Tremella fuciformis*, also known as white jelly mushroom, is an important edible and medicinal fungus containing abundant biologically active polysaccharides [6]. During its cultivation process, the growth and development

of *T. fuciformis* fruiting bodies is extremely dependent on exogenous nutrients supplied by its companion *Annulohypoxylon* species via degrading biomass substrate. Among the companion strains, the fungus of *Annulohypoxylon stygium* is the preferred one, which belongs to Xylariaceae, Ascomycota [7,8]. The companion strains, especially *A. stygium*, have been shown to perform well in lignin and carbohydrate degradation with various glycohydrolases, including pectinases, xylanases, and β-glucanases [9,10]. Moreover, it is indicated that the xylanases secreted by companion *Annulohypoxylon* species possess higher activity in comparison to those from other edible fungi [11]. However, the genes encoding the xylanases from companion *Annulohypoxylon* species have yet to be revealed.

T. fuciformis, with its companion strains, constitutes one microbiota in which the majority of these microorganisms have not yet been isolated and identified, thus resulting in a limit on the mining of the xylanase genes. Metagenome sequencing and screening are effective tools, and can be used to search for and identify some novel target enzymes [12]. Several novel xylanases have been identified by metagenomics studies of camel rumen, chicken cecum, termite hindgut, and cow manure [13–16]. Furthermore, heterologous expressions of these xylanases identified in different hosts by genetic engineering technology could efficiently improve the xylanase yields and exhibit their high thermostability, catalytic efficiency, and organic solvent tolerance [17].

In this study, the microbiota of *T. fuciformis* with its companion strains were used to perform metagenomics sequencing, and the metagenomics data were used to mine novel xylanase enzymes. Three xylanase candidates were screened and predicted based on genomic annotation in combination with their three-dimensional structure modeling. Furthermore, heterologous expression in two different hosts of *E. coli* and *P. pastoris* confirmed that the three candidate enzymes possessed xylanase activities. The three recombinant enzymes were purified and characterized for their enzymatic properties. This is the first report on the xylanase enzymes derived from *T. fuciformis* with its companion strains.

2. Results and Discussion

2.1. Analysis of Metagenomic Sequencing

In our previous study, *T. fuciformis* with its companion strains showed a stronger ability to secrete xylanase than other edible fungi. However, the majority of the microbiota have not yet been isolated and identified, which resulting in the difficulty of identifying these xlyanase genes. Herein, the metagenomic sequencing method was used to search the potential xylanase enzymes in the microbiota of *T. fuciformis* and its companion strains. The metagenomics DNA was extracted from the mycelium of *T. fuciformis* with its companion strains by the CTAB method, and the extracted DNA quality was assessed by agarose gel electrophoresis. As shown in Figure 1A, the extracted DNA band was clear and bright, with a size of more than 8000 bp, and no tailing could be observed, suggesting that the metagenomic DNA quality satisfied the sequencing demand. The raw data of metagenomics sequencing generated 62,890,030 reads, which were treated via assembly, CDS prediction, and redundancy elimination. The sum of the unigenes with full open reading frames reached 50,904, which occupied 72.17% of the total unigenes and exhibited good fitness. The taxonomic profile of the microbiota, as deduced from the raw data, is visualized in Figure 1C. The results revealed that the microbiota of *T. fuciformis* with its companion strains contained 55% prokaryotes, 29% eukaryota, and 16% unclassified species, respectively. Among the prokaryotic microorganisms, *Sphingobacterium thalpophilum* and *Achromobacter sp.* were the dominant bacteria, with the fractions of 19% and 9%, respectively, while the fungi of *Eutypa lata*, *Pestalotiopsis lata*, and *Annulohypoxylon stygium* as the main species occupied 7%, 5%, and 5% of the eukaryotic microorganisms, respectively. Furthermore, the obtained unigenes underwent BLASTp alignment with protein sequence from the CAZy database, which resulted in 199 unigenes annotated and classified according to enzyme function (Figure 1B). A total of 84 unigenes among the 199 annotated unigenes were predicted as glycoside hydrolase (GH) and exhibited the largest proportion

of CAZymes, with 42.2%, demonstrating that a large amount of GH enzymes might be secreted by *T. fuciformis* with its companion strains.

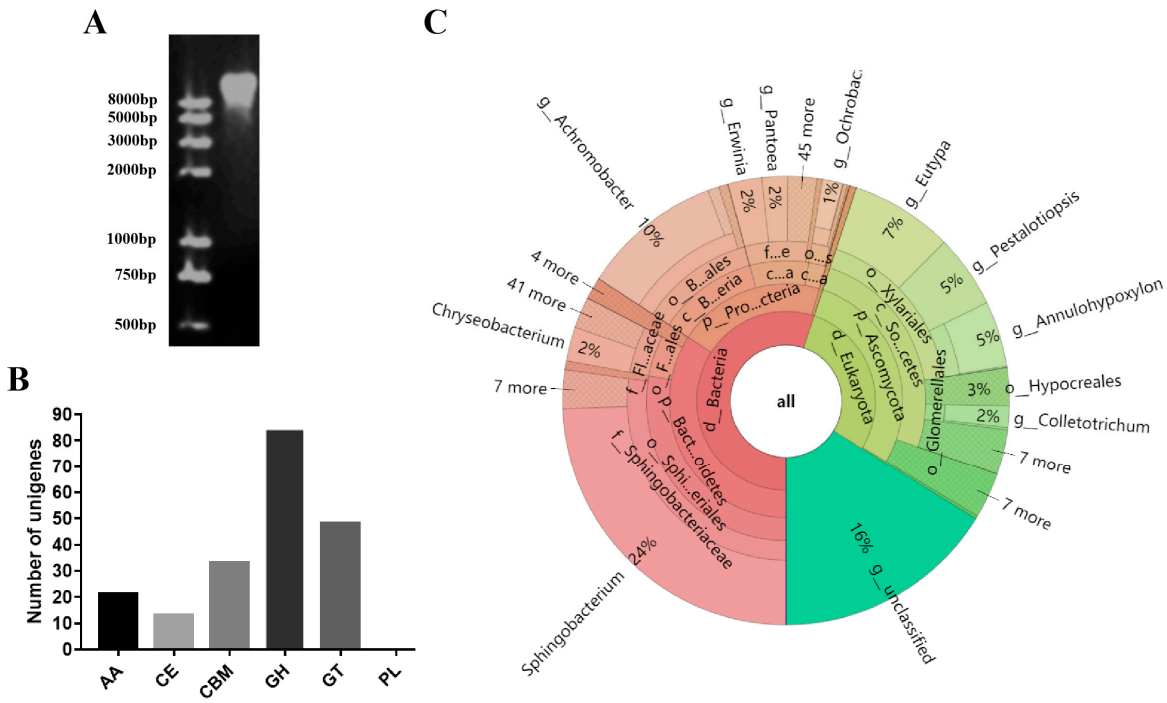

Figure 1. Analysis of metagenomics sequencing. (**A**) Analysis of extracted metagenomic DNA. (**B**) CAZy classification statistics. (**C**) Krona species annotation.

2.2. In Silico Screening of Xylanase Condidates

Among the annotated unigenes of 88 GHs, 3 unigenes were predicted as xylanase candidate genes originating from *A. stygium* and *Sphingobacterium sp,.* respectively (Table 1). BLASTp's alignment with the CAZy database by DIAMOND software indicated that the unigenes of 11,018 and 14,634, designated as *As*Xyn1 and *As*Xyn2, shared the identities of 97% and 100% with those from *A. stygium*, which belonged to the GH10 and GH11 xylanase families, respectively. On the other hand, the unigene of 52,146, designated as *Ss*Xyn, shared a 95% identity with the GH10 family xylanase from *Sphingobacterium* sp.

Table 1. Candidate xylanase genes predicted by metagenomic sequencing.

Unigene	Name	Gene Annotation	Strain	Family	Gene Length	Identity
11,018	*As*Xyn1	xylanase	*A. stygium*	GH10	1110	97%
14,634	*As*Xyn2	xylanase	*A. stygium*	GH11	651	100%
52,146	*Ss*Xyn	xylanase	*Sphingobacterium* sp.	GH10	1149	95%

To obtain the exact sequence information of xylanase ORFs, the total RNA extraction of the microbiota was performed and used as the template with which to generate the cDNA via the RT-PCR method. Three genes encoding the xylanase candidates of *As*Xyn1, *As*Xyn2, and *Ss*Xyn were PCR-amplified using the cDNA as the template by the corresponding primers designed according to their unigene sequences. The sequencing results showed that the *As*Xyn1 gene had a size of 984 bp and encoded 327 amino acids, which was smaller than the size of the *As*Xyn1 gene (1110 bp) from genomic DNA. Sequence alignment indicated that the ORF of *As*Xyn1 gene from genomic DNA contained 2 introns (Table S1), while the genes of *As*Xyn2 and *Ss*Xyn had sizes of 651 bp and 1149 bp and encoded 216 and 382 amino acids, respectively, which was consistent with their unigene sequences

(Table S1). Furthermore, the structures of three xylanase candidates were predicted by the SWISS-MODEL web server with the best matching templates of xylanase structures (PDB ID: 1K6A for *As*Xyn1, 3WP3 for *As*Xyn2, and 4K68 for *Ss*Xyn), which were used to confirm their potential functions. As shown in Figure 2A,C, the overall structures of *As*Xyn1 and *Ss*Xyn fit the typical (β/α)8-barrel skeleton, and two conserved residues of Glu155 and Glu262 for *As*Xyn1 (Glu166 and Glu271 for *Ss*Xyn) could be observed in the active pocket as acid/base catalytic residues. The shape of the overall *As*Xyn2 structure appeared as a "right hand" composed of β-sheets and α-helix, and the β-sheets formed the "palm" and "fingers", with an angle of nearly 90 degrees. Two active residues of Glu110 and Glu201 as general acid/base catalytic sites were located in this catalytic center region (Figure 2B). The observed information represented the typical characteristics of GH10 family xylanase for *As*Xyn1 and *Ss*Xyn and GH11 family xylanase for *As*Xyn2, suggesting that the three xylanase candidates had potential xylanase activity [18,19].

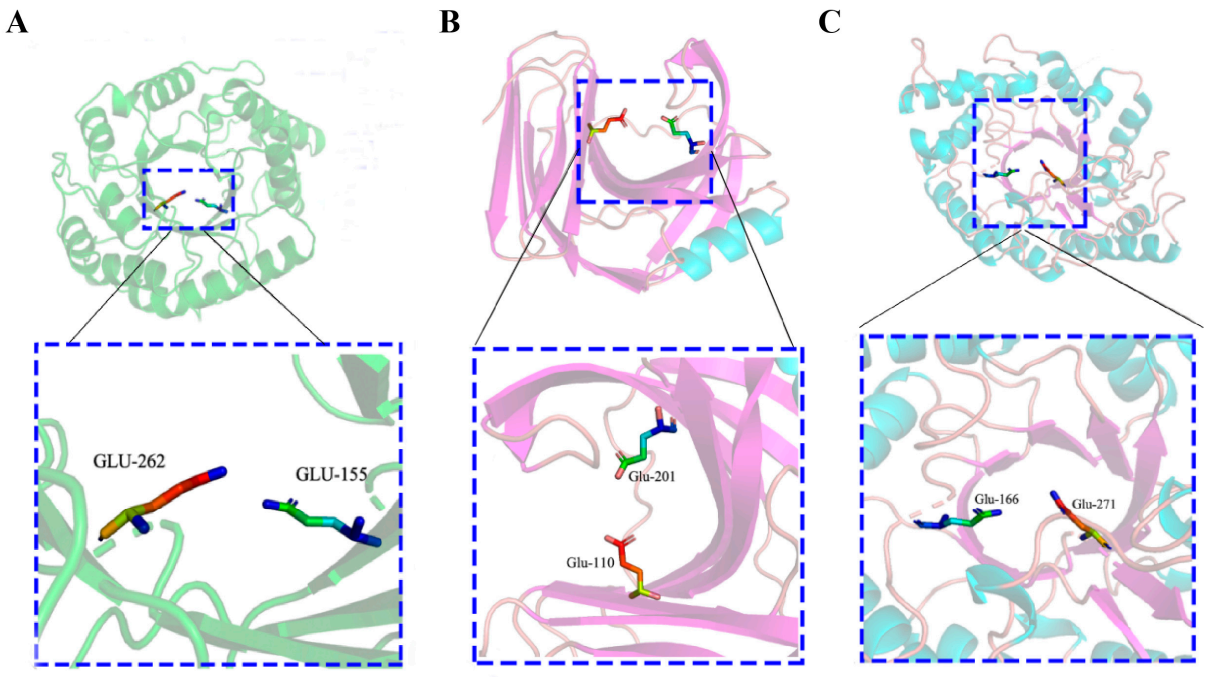

Figure 2. Analysis of tertiary structure for three xylanase candidates. (**A**) *As*Xyn1; (**B**) *As*Xyn2; (**C**) *Ss*Xyn.

2.3. Expression of the Xylanase Candidates in E. coli and P. pastoris

To express the mature enzymes of three xylanase candidates, their signal peptides were predicted and removed by a SignalP 4.1 server (https://services.healthtech.dtu.dk/services/SignalP-4.1/, accessed on 1 February 2020) (Table S2). Subsequently, three mature genes were PCR-amplified and ligated into the pET-28a plasmid to develop expression vectors of pET-28a-*As*Xyn1, pET-28a-*As*Xyn2, and pET-28a-*Ss*Xyn, which were transformed into *E. coli* BL21 (DE3) for enzyme expression. The expression level and solubility of the recombinant enzymes were analyzed by SDS-PAGE. As shown in Figure 3A, three clear bands of the recombinant enzymes could be observed in SDS-PAGE gel, showing that the candidate enzymes were expressed successfully in *E. coli*. Furthermore, the solubility of the recombinant enzymes was analyzed as shown in Figure 3B,C. The results indicated that the recombinant enzyme of *Ss*Xyn from *Sphingobacterium* sp. appeared to have soluble expression with a small amount of inclusion body, and a relatively high activity of 14.36 U/mL was detected by the *Ss*Xyn crude enzyme, which was used for purification and further biochemical characterization. On the contrary, the recombinant enzymes of *As*Xyn1 and *As*Xyn2 were mainly expressed as inclusion bodies, and less soluble proteins can be observed in Figure 3B. Low activities of crude enzymes were also detected for 0.06 U/mL

of *As*Xyn1 and 0.16 U/mL of *As*Xyn2, respectively, partially due to low soluble expression (Figure 3D). A possible explanation is that the enzymes of *As*Xyn1 and *As*Xyn2 from the fungus *A. stygium* were not suitable for the expression system of *E. coli*. To overcome the insoluble expression of *As*Xyn1 and *As*Xyn2 in *E. coli*, the two genes without signal peptides were ligated into the expression pPIC9K vector and transformed into *E. coli* DH5α. The recombinant vectors were subsequently linearized and transformed into *P. pastoris* GS115 for genomic integration. The obtained transformants with different copies were screened using fresh YPD medium containing 0–4.0 mg/mL geneticin, as shown in Figure 4. The multi-copy transformants were randomly selected and cultivated in BMGY medium for induced expression by methanol. The culture supernatants containing secreted enzymes were used for enzyme activity assays. The results showed that the activities of two recombinant enzymes in the culture supernatants showed increasing trends with the increase in time, and maximum activities of 1.90 U/mL for *As*Xyn1 and 2.11 U/mL *As*Xyn2 could be achieved at 120 h and 96 h, respectively. This indicated that two candidate enzymes were expressed successfully in *P. pastoris* and exhibited xylanase activity.

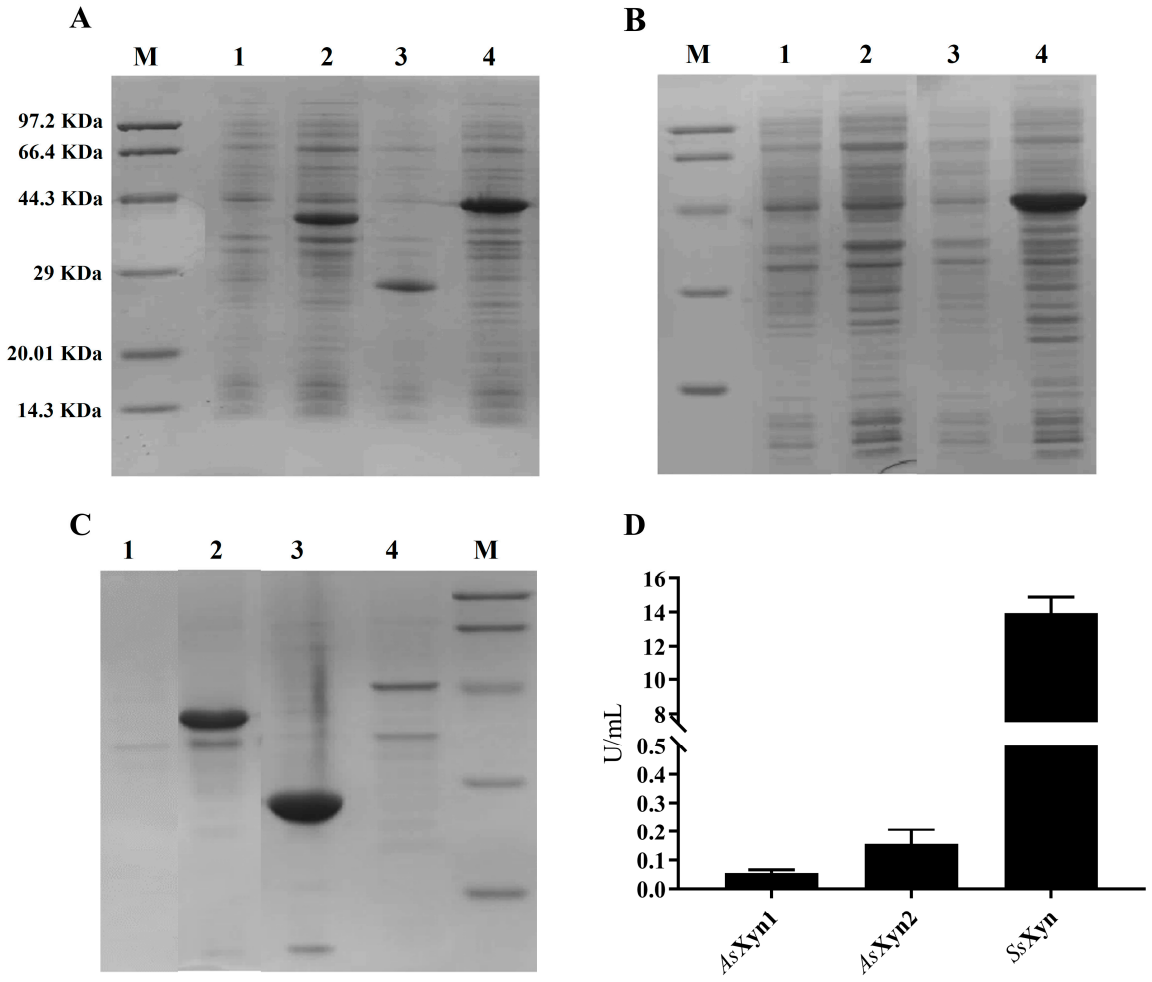

Figure 3. Analysis of expression level and solubility for recombinant enzymes in *E. coli*. (**A**) Whole-cell lysate; (**B**) cell lysate supernatant; (**C**) cell lysate precipitation; (**D**) crude enzyme activity (Lane M: Protein Marker; Lane 1: *E. coli* BL21 (DE3)/pET28a; Lane 2: *E. coli* BL21 (DE3)/pET28a-*AsXyn1*; Lane 3, *E. coli* BL21 (DE3)/pET28a-*AsXyn2*; Lane 4, *E. coli* BL21 (DE3)/pET28a-*SsXyn*).

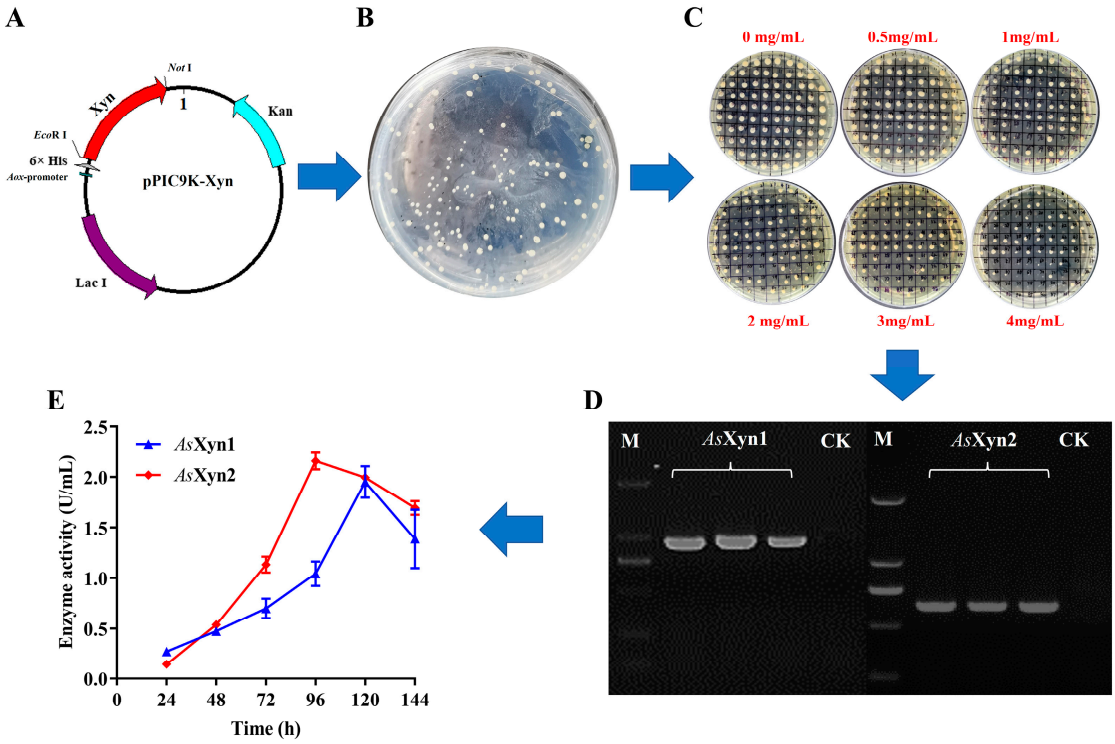

Figure 4. Heterologous expression of *As*Xyn1 and *As*Xyn2 in *P. pastoris*. (**A**) Construction of recombinant plasmid; (**B**) preliminary screening; (**C**) multi-copy transformant selection; (**D**): colony PCR verification; (**E**): activity assays of the supernatants by recombinant *P. pastoris*.

2.4. Characterization of the SsXyn Enzyme in E. coli

The recombinant enzyme of *Ss*Xyn, with a 6×His tag in *E. coli* after sonication, was purified by Ni-Sepharose Histrap HP column and then characterized for its enzymatic properties. The purified *Ss*Xyn enzyme was analyzed by SDS-PAGE, and a clear band with the size of 43.5 kDa can be observed in Figure 5A, indicating that a pure enzyme was obtained. Furthermore, the effects of temperature and pH on the activity of purified *Ss*Xyn enzyme were determined. The results showed that the xylanase activity could be increased with an increase in temperature from 20 °C to 30 °C, and a sharp drop appeared at over 30 °C. A maximum specific activity of 33.1 U/mg could be obtained at 30 °C (Figure 5B). Under the optimum temperature, the *Ss*Xyn enzyme exhibited the highest specific activity of 62.5 U/mg at pH 8.0, and more than 50% of the activity was retained between pH 7.0 and pH 10.0 (Figure 5C). The thermostability analysis indicated that the *Ss*Xyn enzyme possessed better activity at a low temperature (Figure 5B). Moreover, the excellent stability of *Ss*Xyn at pH values from 5.0 to 8.0 could be observed. These results demonstrated that the *Ss*Xyn enzyme was suitable for use at room temperature with a relatively broad pH range [20]. Among all the tested ions, Co^{2+} and Ba^{2+} were able to improve the enzyme activity of *Ss*Xyn by 4% and 10%, respectively. However, obvious inhibition, with an activity decrease of over 40%, could be observed by the ions of Fe^{2+} and Fe^{3+} (Figure 5D). Furthermore, some chemical reagents also affected the enzyme activity of *Ss*Xyn. As shown in Figure 5E, Tween 80 with 10 mM supplemented in the reaction solution efficiently improved its activity, leading to a 50% increase. Kinetics analysis of the *Ss*Xyn enzyme was performed with different concentrations of beechwood xylan at the optimum pH and room temperature, and the results indicated that the estimated values of K_m and V_{max} were 2.9 mg/mL and 65.8 U/mg according to *Ss*Xyn, respectively (Figure 5F).

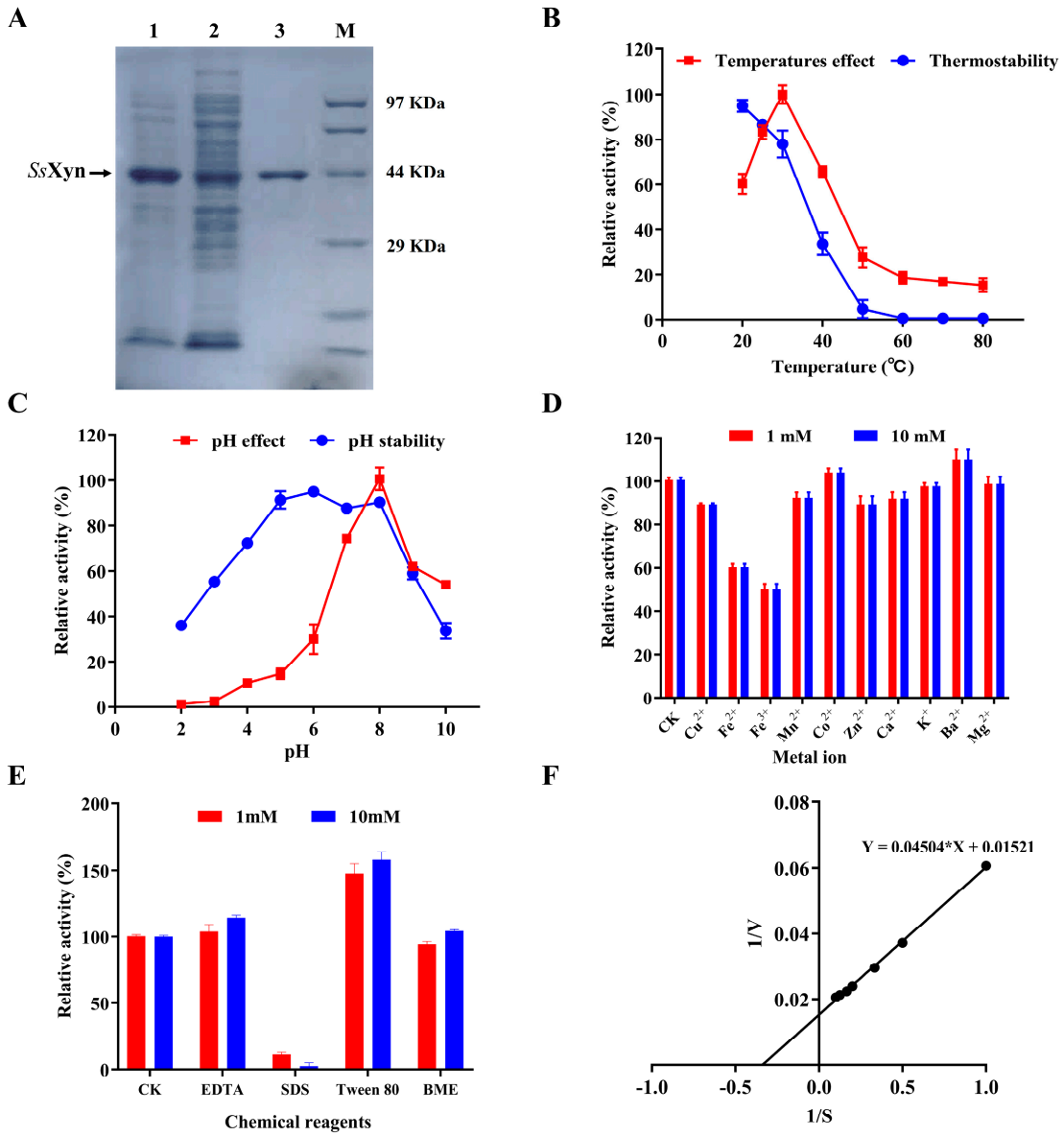

Figure 5. Biochemical characterization of recombinant *Ss*xyn enzyme in *E. coli*. (**A**) Recombinant *Ss*Xyn purification; (**B**) temperature effect and thermostability; (**C**) pH effect and pH stability; (**D**) metal ion effect; (**E**): chemical reagents' effect; (**F**) Lineweaver–Burk diagram of double reciprocal for *Ss*Xyn enzyme (Lane M: protein marker; Lane 1: cell lysate; Lane 2: flowthrough from purification step; Lane 3: purified *Ss*xyn enzyme).

2.5. Characterization of the AsXyn1 and AsXyn2 Enzymes in P. pastoris

The recombinant enzymes of *As*Xyn1 and *As*Xyn2 expressed by *P. pastoris* were purified by the procedure described in "Materials and methods". After purification, the purity levels of two enzymes were analyzed by SDS-PAGE. As shown in Figure 6A, a high purity was achieved by *As*Xyn1, while *As*Xyn2 with partial purification was obtained, as it is not easy to bind Ni resin via a 6-His tag. A possible reason is that the 6-His tag might be buried within the enzyme. The purified enzymes of *As*Xyn1 and *As*Xyn2 showed different specific activities at different temperatures. A maximum specific activity of 84.50 U/mg for *As*Xyn1 could be observed at the optimum temperature of 50 °C, which was close to reported metagenomics GH10 xylanases from chick cecum and the feces of *Rhinopithecus bieti* [14,21]. The optimum temperatures for *As*Xyn2 were observed at 40 °C, and the corresponding specific activities reached 4.8 U/mg (Figure 6C). A low enzyme activity for

*As*Xyn2 was partially ascribed to low enzyme purity. The relatively high thermostability could be determined by the purified enzymes of *As*Xyn1 and *As*Xyn2, which were able to maintain more than 70% activity of the initial activity after incubation at 40 °C for 1 h (Figure 6D). However, both enzymes showed complete inactivation after pre-incubation at over 50 °C for 1 h. In previous studies, several xylanases belonging to families 10 and 11 were identified from chick cecum and *Rhizopus oryzae*, exhibiting higher thermostability at 50 °C [14,22]. Under the corresponding optimum temperatures, maximum specific activities of 120.8 U/mg and 5.3 U/mg for *As*Xyn1 and *As*Xyn2 could be achieved at a pH of 6.0 (Figure 6E). Furthermore, the two enzymes of *As*Xyn1 and *As*Xyn2 exhibited excellent and broad pH stability in the range of 2.0–10.0 (Figure 6F). The *As*Xyn1 enzyme retained over 60% of its initial enzyme activity when it was incubated at pH values from 2.0 to 10.0 for 1 h, and the residual activity of the *As*Xyn2 enzyme could be maintained at more than 70% of initial activity after incubation at a pH of 3.0–10.0 for 1 h. Similar results were also found for families 10 and 11 of xylanses from *Rhizopus oryzae* [22]. A high pH stability could be observed in the range of 4–10 for GH10 xylanase and 4–8 for GH11 xylanase.

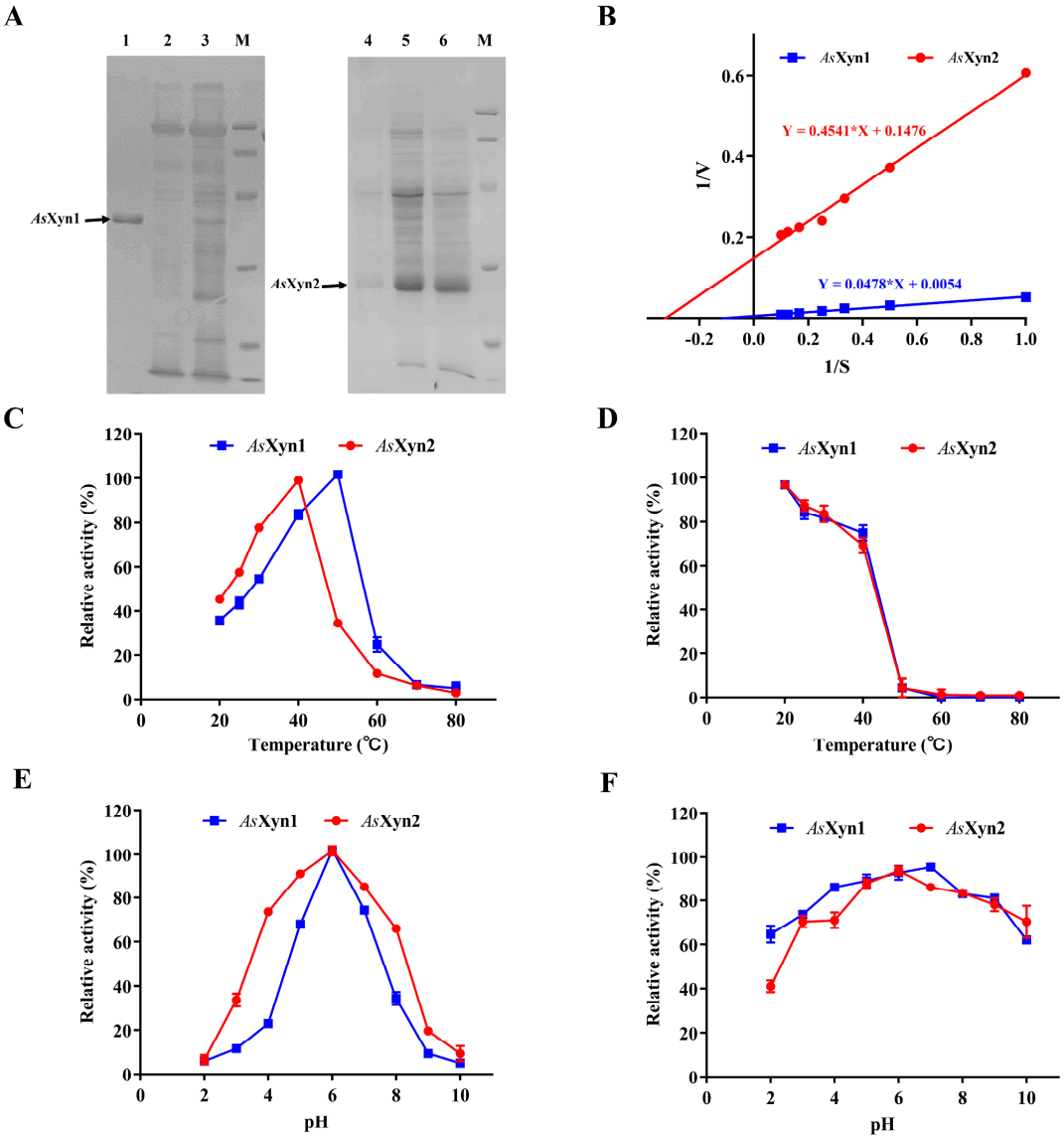

Figure 6. Characterization of the recombinant *As*Xyn1 and *As*Xyn2 enzymes by *P. pastoris*. (**A**) Enzyme purification; (**B**) double reciprocal diagram of recombinant *As*Xyn1 and *As*Xyn2 xylanases; (**C**) temperature effects; (**D**) thermostability; (**E**) pH effects; (**F**) pH stability.

The effects of metal ions and chemical reagents on the activities of *As*Xyn1 and *As*Xyn2 were determined as shown in Table 2. Among all the tested metal ions and chemical reagents, metal ions of Co^{2+}, Ca^{2+}, Ba^{2+}, Mg^{2+}, and Tween 80 at the concentrations of 1 mM or 10 mM could efficiently improve the enzyme activity of *As*Xyn1, with maximum increases of 17.3%, 16.0%, 29.7%, 12.0%, and 27.7%, respectively (Table 2). On the other hand, the *As*Xyn2 enzyme could only be activated by Tween 80 at 10 mM, with an increase of 27.0%. In addition, the *As*Xyn1 enzyme was shown to be significantly sensitive to Cu^{2+}, Fe^{3+}, and SDS, and resulted in enzyme inactivation. On the contrary, the *As*Xyn2 enzyme possessed better tolerances to all the tested metal ions than *As*Xyn1 did. These results demonstrated the property differences of xylanases between the GH10 family and the GH11 family. Furthermore, the kinetics of the *As*Xyn1 and *As*Xyn2 enzymes were assayed under the optimum pH value at room temperature by using different birchwood xylan concentrations. The kinetic parameters of K_m and V_{max} were calculated to be 8.9 mg/mL and 185.2 U/mg for *As*Xyn1, and 3.1 mg/mL and 6.8 U/mg for *As*Xyn2 (Figure 6B).

Table 2. Effects of metal ions and chemical reagents on the activities of recombinant xylanases.

Metal Ions and Chemical Reagents	Relative Activity (%)			
	***As*Xyn1**		***As*Xyn2**	
	1 mM	**10 mM**	**1 mM**	**10 mM**
Control	100.0 ± 0.7	100.0 ± 0.9	100.0 ± 1.1	100.0 ± 0.9
Cu^{2+}	16 ± 1.6	2 ± 0.4	95 ± 2.0	41 ± 1.6
Fe^{2+}	54 ± 2.9	41 ± 0.4	76 ± 3.3	12 ± 1.3
Fe^{3+}	21 ± 1.8	4 ± 2.7	81 ± 2.2	46 ± 1.8
Mn^{2+}	75 ± 2.0	75 ± 2.0	68 ± 2.7	55 ± 1.8
Co^{2+}	110 ± 8.0	117 ± 4.4	89 ± 2.2	63 ± 1.8
Zn^{2+}	71 ± 0.4	40 ± 1.6	91 ± 1.1	60 ± 1.6
Ca^{2+}	111 ± 6.2	116 ± 3.3	94 ± 1.6	95 ± 1.8
K^{+}	101 ± 5.1	103 ± 7.3	94 ± 3.1	98 ± 1.1
Ba^{2+}	109 ± 3.3	130 ± 3.8	94 ± 2.0	96 ± 1.3
Mg^{2+}	111 ± 4.9	112 ± 4.7	97 ± 1.3	97 ± 1.3
EDTA	83 ± 3.1	64 ± 2.9	85 ± 3.6	69 ± 6.7
SDS	4 ± 1.3	2 ± 1.6	84 ± 1.3	2 ± 1.1
Tween 80	115 ± 2.7	128 ± 14.4	95 ± 1.6	127 ± 5.3
BME	108 ± 1.6	80 ± 5.3	88 ± 1.3	78 ± 2.7

The above enzymatic properties of *As*Xyn1 and *As*Xyn2 were similar to those of xylanase purified from spent mushroom compost (SMC) of *T. fuciformis* in our previous study [11]. Combined with the molecule weight, the *As*Xyn1 enzyme mined from metagenomic data should have been the same as the xylanase reported in our previous study [11]. However, the activity of the recombinant *As*Xyn1 enzyme in *P. pastoris* was obviously lower than that of xylanase purified from the SMC of *T. fuciformis*. Moreover, the kinetic parameters and thermostability had changed between them [11]. Therefore, we repeated the purification of xylanase from SMC of *T. fuciformis* and performed a commercial mass spectrum assay. The results of the analysis indicated that the sequence of purified xylanase was consistent with that of *As*Xyn1 enzyme. Furthermore, we found that the molecular weight of *As*Xyn1 expressed in *P. pastoris* was slight higher than that of *E. coli* (Figures 3 and 6). A possible explanation is that glycosylation of the *As*Xyn1 enzyme by *P. pastoris* led to reduced activity when compared with the wild xylanse enzyme from SMC. Thus, a deglycosylation experiment of the recombinant *As*Xyn1 enzyme expressed by *P. pastoris* was carried out (Figure 7). The activity of *As*Xyn1 enzyme after deglycosylation with 62.3 U/mg was obtained under optimal conditions, while the recombinant *As*Xyn1 enzyme exhibited higher activity of 120.8 U/mg. These results suggest that glycosylated modification of the *As*Xyn1 enzyme had an important impact on its activity, although the post-translational modification of the *As*Xyn1 enzyme in a wild strain not yet known.

Previous studies have shown that protein glycosylation plays a key role in the regulation of enzyme activity [23–25]. Moreover, the covalent addition of glycans to the enzyme surface could modulate the kinetic parameters and thermostability [26]. The xylanase from *Bacillus subtilis* was engineered by protein glycosylation, which revealed its improved thermostability [24]. In this study, the results show that a significant reduction in enzyme activity and thermostability for *As*Xyn1 expressed by *P. pastoris* could be observed in comparison to that of a wild strain. A comprehensive understanding of the potential mechanism between them would favor the design of an enzyme with higher enzymatic activity and thermostability.

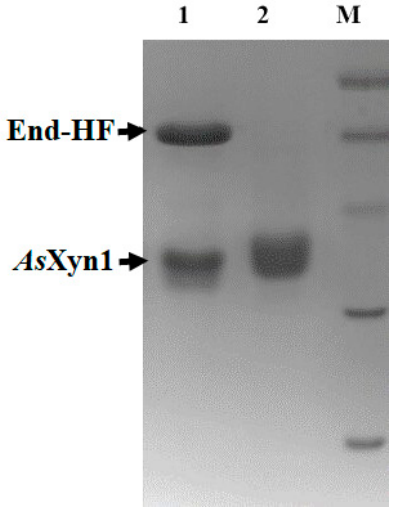

Figure 7. Deglycosylation of the recombinant *As*Xyn1 enzyme by End-HF enzyme. Lane M: protein marker; Lane 1: deglycosylation of *As*Xyn1; Lane 2: *As*Xyn1 as control.

3. Materials and Methods

3.1. Strains and Plasmids

The microbiota of *T. fuciformis* with its companion strains was obtained from the Bioengineering Training Center, Fujian Agriculture and Forestry University (Fujian, China). The *E. coli* DH5a strain was used as the cloning host for plasmid construction, while the *E. coli* BL21(DE3) strain was used as an expression host for the heterologous expression of the xylanase candidates using expression vector Novagen® pET28a-(+) (Darmstadt, German). The *P. pastoris* GS115 strain was used as the expression host for the heterologous expression of the xylanase candidates via expression vector pPIC9K.

3.2. Metagenomic DNA Extraction and Analysis

The microbiota of *T. fuciformis* with its companion strains was inoculated into a liquid substrate medium (20 g/L sawdust, 5 g/L wheat bran, 2 g/L NaCl, 0.5 g/L $MgSO_4$, and 0.5 g/L KH_2PO_4) and cultured in the dark at 25 °C. The mycelia were collected and ground with liquid nitrogen using a mortar. The metagenomic DNA extraction was performed using the CTAB method and stored at −80 °C. Subsequently, metagenomic DNA was stored in dry ice and send to a commercial company for metagenomic sequencing. Read-based metagenomic analysis was carried out using the software metaSPAdes 3.11.0. The NR database was employed for species annotation, and extraction sequences belonging to microorganisms from the NR database formed the NR_meta sublibrary. DIAMOND software (https://github.com/bbuchfink/di, accessed on 1 February 2020) was used to compare the above unigenes in the NR_meta sublibrary, combined with the NCBI species classification database, realizing species-specific annotation information for each taxonomic level of the sequence.

3.3. Sequence Analysis

The unigenes obtained from sequencing were aligned with the protein sequence in the CAZy database using DIAMOND software (blastp, evalue $\leq 1 \times 10^{-5}$). The highest alignment scores were used for the protein annotations. According to the annotations, the unigene number distribution information of six functional enzymes in the metagenome was calculated according to the CAZy database. Unigenes annotated as xylanase were searched for among the CAZy annotation results. The amino acid sequences encoded by the putative xylanase genes were analyzed by BioEdit software 7.0.9 to identify ORFs, and this was further confirmed using the NCBI BLASTp algorithm (https://blast.ncbi.nlm.nih.gov/Blast.cgi, accessed on 1 February 2020). Physical and chemical properties, including molecular weight, isoelectric point, etc., of the assigned protein were analyzed by the ProtParam (https://web.expasy.org/protparam/, accessed on 1 February 2020). Selected putative xylanases were structurally modeled through the SWISS-MODEL web server (https://swissmodel.expasy.org/interactive, accessed on 1 February 2020) with the best matching template, and protein structures were visualized and analyzed using PyMol 2.4 software.

3.4. RNA Extraction and cDNA Amplification

The microbiota of *T. fuciformis* with its companion strains was inoculated into a liquid substrate medium and cultured in the dark at 25 °C for 7~9 d. The mycelia were collected, and total RNA extraction was performed via the Trizol method. In order to obtain the cDNA of the xylanase-encoding gene, the reverse transcriptase (RT-PCR) technique was used to synthesize the cDNA via Takara's Prime Script® RT regent Kit (Takara, Dalian, China) with gDNA Eraser. Candidate xylanase genes were amplified by the prepared cDNA, as the template using the corresponding primers was designed according to metagenomic sequencing results (Table 3). The designed primers are given in Table 1. The PCR amplification reactions consisted of 0.5 ng of cDNA, 1 × TransStart Fast Pfu Buffer, 0.2 mM dNTP, 0.2 μM forward and reverse primers, and 1 unit of Fast Pfu DNA Polymeras (TransGen). The PCR products were analyzed using 1% agarose gel and subsequently purified with the AxyPrep DNA Gel Extraction Kit for commercial sequencing, obtained from Sangon Biotech (Shanghai, China).

Table 3. Primer sequences used in this study.

Name	Primer Sequence (5′→3′)
28a-*As*Xyn1-F	GGACAGCAAATGGGTCGCGGATCCGCCGACAGCATCGACGCCTT
28a-*As*Xyn1-R	TGGTGCTCGAGTGCGGCCGCAAGCTTTTTCAGGGCGTTCACGACAG
28a-*Ss*xyn-F	GGACAGCAAATGGGTCGCGGATCCAATATACAGGATCTGGAACA
28a-*Ss*xyn-R	GTGGTGCTCGAGTGCGGCCGCAAGCTTCTTTTTTTTTTGAGTCAATG
28a-*As*Xyn2-F	GGACAGCAAATGGGTCGCGGATCCTCGCCGCTCGACCTAATCAC
28a-*As*Xyn2-R	TGCTCGAGTGCGGCCGCAAGCTTAGACTGCTCAACGGTAATC
9k-*As*Xyn1-F	GCTGAAGCTTACGTAGAATTCCATCATCACCATCACCACGCCGACAGCATCGACGCCTT
9k-*As*Xyn1-R	AGGCGAATTAATTCGCGGCCGCTTTCAGGGCGTTCACGACAG
9k-*As*Xyn2-F	CTGAAGCTTACGTAGAATTCTCGCCGCTCGACCTAATCAC
9k-*As*Xyn2-R	GCGAATTAATTCGCGGCCGCATGATGATGATGATGATGAGACTGCTCAACGGTAATC

3.5. Heterologous Expression of the Putative Xylanase Candidates in E. coli

The PCR amplification products of the xylananse candidates were ligated to the pET-28a expression vector by homologous recombination to generate the recombinant plasmids, which were transformed into *E. coli* DH5α-competent cells. The obtained recombinant strains were used to perform commercial sequencing to confirm the correct construction. Subsequently, the recombinant plasmids were extracted and transformed into *E. coli* BL21 (DE3), resulting in the recombinant expression strains. For heterologous expression, the recombinant *E. coli* BL21 (DE3) strains harboring the expression vectors were cultured in 50 mL LB medium containing kanamycin (50 μg/mL) at 37 °C and 180 rpm for 2.5 h,

and IPTG, as an inducer, with a final concentration of 0.5 mM was added into the broth to induce the protein expression at 18 °C and 180 rpm overnight. The induced cells were harvested by centrifugation at 4 °C and 6000× *g* for 10 min, then resuspended in 100 mM phosphate buffer (pH 8.0). After sonication on ice and centrifugation at 4 °C, the supernatant and precipitation were collected to analyze the expression level and solubility of the recombinant proteins through SDS-PAGE.

3.6. Heterologous Expression of the Putative Xylanase Candidates in P. pastoris

The PCR amplification products of the xylananse candidates were ligated to the pPIC9K plasmid by means of homologous recombination to develop the recombinant plasmids, which were transformed into *E. coli* DH5α-competent cells for commercial sequencing. The correct recombinant plasmids were linearized by restriction endonuclease of EcoR I or Not I, and then transformed into *P. pastoris* GS115 by electroporation. The cell suspensions, after transformation, were spread and grown on the MD plates for 2~3 days to select positive transformants at 30 °C. Multicopy transformant selection of *P. pastoris* was performed on YPD plates containing 1.0–4.0 mg/mL geneticin. The positive transformants with high resistance to geneticin were randomly selected and confirmed by colony PCR, and *P. pastoris* transformed with the empty pPIC9K vector was used as the control. For heterologous expression, the *P. pastoris* transformants were inoculated into BMGY medium and grown at 30 °C and 180 rpm until the OD value at 600 nm reached 2.0~6.0. The cells were harvested by centrifugation at 5000× *g* for 10 min and resuspended to the OD_{600} of 1.0 using fresh BMMY medium. Subsequently, methanol was supplemented to 0.5% of the final concentration every 24 h to induce the protein expression until 120 h. During the induction process, the samples were taken each 24 h to evaluate the protein expression via by SDS-PAGE and assay the enzyme activity.

3.7. Purification of Recombinant Enzymes

The recombinant *E. coli* cells were resuspended in lysis buffer (50 mM phosphate, 300 mM NaCl, 10 mM imidazole, pH 8.0) and disrupted by sonication on ice. The supernatant, as the crude enzyme after centrifugation, was loaded into a Ni-Sepharose Histrap HP column. The pre-cooling wash buffer (50 mM phosphate, 300 mM NaCl, 50 mM imidazole, pH 8.0) was used to remove non-specific proteins, and a linear gradient elution with pre-cooling elution buffer (50 mM phosphate, 300 mM NaCl, 50–500 mM imidazole, pH 8.0) was performed to obtain the pure target enzyme. The eluate containing the pure enzyme was desalted and concentrated using a 10 kDa cut-off Centriprep device (GE Health-care, Chicago, IL, USA). For the purification of recombinant enzymes by *P. pastoris*, the culture supernatant collected by centrifugation was precipitated using 80% ammonium sulfate saturation. The precipitated protein was obtained by centrifugation and resuspended using ultrapure water. A Centriprep device with 10 kDa cut-off was used for the desalination and concentration of the protein sample, which was subsequently subjected to enzymatic purification using a Ni-Sepharose Histrap HP column (GE Health-care, Chicago, IL, USA), as mentioned for the above method. These purified enzymes were stored at −20 °C for further experiments.

3.8. Enzyme Activity Assays

The xylanase activity was assayed by measuring the production of reducing sugar from the hydrolysis of beechwood xylan using the DNS method. The reaction mixture contained 375 μL 1% (*w*/*v*) beechwood xylan and the appropriate enzyme solution in 500 μL sodium acetate buffer (50 mM, pH 5.2). The reaction mixture was maintained for 30 min, and the reaction was stopped with 750 μL of DNS solution. The changes in absorbance were detected at the wavelength of 540 nm using a spectrophotometer (UV-1800, Mapada, Shanghai, China), and the xylose concentration was quantified according to the calibration curve of standard xylose. One unit (U) of xylanase activity is defined as the amount of enzyme required to produce 1 μmol of xylose in 1 min. The protein

concentrations of crude and purified enzymes were quantified using the Brandford method. All the experiments were performed in triplicate.

3.9. Characterization of Recombinant Enzymes

The effects of temperature and pH on the activities of recombinant xylanases were conducted in the range of 20–80 °C and pH 2.0–10.0. The activities of the purified enzymes were determined at different temperatures using the reaction mixture (50 mM sodium acetate buffer, pH 5.2), and the enzyme activity at an optimum temperature was used as 100%. For the pH effects, the purified enzyme activity was determined by using different buffers. The buffers used in this study included glycine-HCl (50 mM, pH 2.0–3.0), sodium acetate (50 mM, pH 4.0–5.0), sodium phosphate (50 mM, pH 6.0–8.0), and NaOH-glycine (50 mM, pH 9.0–10.0), and the maximum enzyme activity at an optimum pH value was used as 100%. For the enzymatic thermostability, the recombinant xylanase was pre-incubated at different temperatures (20–80 °C) at the optimum pH for 1 h, and the residual enzyme activity was determined at the optimal temperature and pH value. The percentage of the initial activity assayed before pre-incubation under the optimum conditions was calculated as the relative activity at different temperatures. The pH stability assay was determined by pre-incubation of the recombinant xylanase at different pH values of 2.0–10.0 at room temperature for 1 h, and the residual activity was assayed under the optimum temperature and pH value. Similarly, the relative activity was calculated as a percentage of the initial activity assayed before pre-incubation under optimum conditions, which represented 100% enzyme activity. All of the tests were carried out in triplicate.

The substrate concentration of beechwood xylan varied, ranging from 1 to 10 mg/mL, and was used to determine the kinetic constants of recombinant enzymes under the optimum pH value at room temperature. The apparent K_m and V_{max} values were obtained using the Lineweaver–Burk plot for enzymatic reactions, with 1/V and 1/S as coordinates.

4. Conclusions

In this study, three xylanase genes were identified by the metagenomic sequencing method combined with analysis of the protein tertiary structure from the microbiota of *T. fuciformis* and its companion strains. Heterologous expression indicated that, among the three enzymes, *As*Xyn1 possessed high thermostability at 40 °C and broad pH tolerance at the range of 2.0–10.0, exhibiting its application potential. Furthermore, we found that post-translational modification (such as glycosylation) of the *As*Xyn1 enzyme modulated its activity, kinetic parameters, and thermostability. These results and findings provide a hint for future enzyme modification and design.

Supplementary Materials: The following supporting information can be downloaded at: https://www.mdpi.com/article/10.3390/catal14010015/s1, Table S1: Sequence information of the genes identified in this study; Table S2: Analysis of signal peptides for the xylanases identified in this study.

Author Contributions: L.Z. and H.L. conceived this study and designed the experiments; Y.L. and C.L. performed the analysis of metagenome data and developed all the recombinant strains; Y.L. and C.W. determined the enzyme activity; H.L. and L.Z. wrote and edited the manuscript. All authors have read and agreed to the published version of the manuscript.

Funding: This work was supported by the Fujian Science and technology support program (No.2020S0062).

Data Availability Statement: Data are contained within the article and supplementary materials.

Conflicts of Interest: The authors declare no conflict of interest.

References

1. Loqué, D.; Scheller, H.V.; Pauly, M. Engineering of plant cell walls for enhanced biofuel production. *Curr. Opin. Plant Biol.* **2015**, *25*, 151–161. [CrossRef] [PubMed]
2. Miao, Y.; Li, J.; Xiao, Z.; Shen, Q.; Zhang, R. Characterization and identification of the xylanolytic enzymes from *Aspergillus fumigatus* Z5. *BMC Microbiol.* **2015**, *15*, 126. [CrossRef] [PubMed]
3. Bosetto, A.; Justo, P.I.; Zanardi, B.; Venzon, S.S.; Graciano, L.; dos Santos, E.L.; Simão Rde, C. Research Progress Concerning Fungal and Bacterial β-Xylosidases. *Appl. Biochem. Biotechnol.* **2016**, *178*, 766–795. [CrossRef] [PubMed]
4. Moreira, L.R.; Filho, E.X. Insights into the mechanism of enzymatic hydrolysis of xylan. *Appl. Microbiol. Biotechnol.* **2016**, *100*, 5205–5214. [CrossRef] [PubMed]
5. Ariaeenejad, S.; Maleki, M.; Hosseini, E.; Kavousi, K.; Moosavi-Movahedi, A.A.; Salekdeh, G.H. mining of camel rumen metagenome to identify novel alkali-thermostable xylanase capable of enhancing the recalcitrant lignocellulosic biomass conversion. *Bioresour. Technol.* **2019**, *281*, 343–350. [CrossRef] [PubMed]
6. Yuan, H.J.; Dong, L.; Zhang, Z.Y.; He, Y.; Ma, X. Production, structure, and bioactivity of polysaccharide isolated from *Tremella fuciformis*. *Food Sci. Hum. Well* **2022**, *11*, 1010–1017. [CrossRef]
7. Liu, D.M.; Zhu, H.Y.; Pujiana, D.; Zheng, L.S.; Chen, L.G.; Ma, A.M. Cloning and functional characterization of *gpd* and *α-tubulin* promoters from *Annulohypoxylon stygium*, a companion fungus of *Tremella fuciformis*. *Mycoscience* **2020**, *61*, 1–8. [CrossRef]
8. Deng, Y.; Hsiang, T.; Li, S.; Lin, L.; Wang, Q.; Chen, Q.; Xie, B.; ming, R. Comparison of the mitochondrial genome sequences of six *Annulohypoxylon stygium* isolates suggests short fragment insertions as a potential factor leading to larger genomic size. *Front. Microbiol.* **2018**, *9*, 2079. [CrossRef]
9. Robl, D.; Delabona Pda, S.; Mergel, C.M.; Rojas, J.D.; Costa Pdos, S.; Pimentel, I.C.; Vicente, V.A.; da Cruz Pradella, J.G.; Padilla, G. The capability of endophytic fungi for production of hemicellulases and related enzymes. *BMC Biotechnol.* **2013**, *13*, 94. [CrossRef]
10. Wingfield, B.D.; Bills, G.F.; Dong, Y.; Huang, W.; Nel, W.J.; Swalarsk-Parry, B.S.; Vaghefi, N.; Wilken, P.M.; An, Z.; de Beer, Z.W.; et al. IMA Genome-F 9: Draft genome sequence of *Annulohypoxylon stygium*, *Aspergillus mulundensis*, *Berkeleyomyces basicola* (syn. Thielaviopsis basicola), *Ceratocystis smalleyi*, two *Cercospora beticola* strains, *Coleophoma cylindrospora*, *Fusarium fracticaudum*, *Phialophora cf. hyalina*, and *Morchella septimelata*. *IMA Fungus* **2018**, *9*, 199–223.
11. Lin, H.; Sun, M.; Li, J.; Xu, Q.; Yang, B.; Wang, Q.; Xie, W.; Sun, S.; Hu, K.; Zhang, L. Purification and Characterization of Xylanase from Spent Mushroom Compost and its Application in Saccharification of Biomass Wastes. *Bioresources* **2018**, *13*, 220–230. [CrossRef]
12. Hu, Y.; Zhang, G.; Li, A.; Chen, J.; Ma, L. Cloning and enzymatic characterization of a xylanase gene from a soil-derived metagenomics library with an efficient approach. *Appl. Microbiol. Biotechnol.* **2008**, *80*, 823. [CrossRef] [PubMed]
13. Ariaeenejad, S.; Hosseini, E.; Maleki, M.; Kavousi, K.; Moosavi-Movahedi, A.A.; Salekdeh, G.H. Identification and characterization of a novel thermostable xylanase from camel rumen metagenome. *Int. J. Biol. Macromol.* **2019**, *1*, 1295–1302. [CrossRef] [PubMed]
14. Al-Darkazali, H.; Meevootisom, V.; Isarangkul, D.; Wiyakrutta, S. Gene expression and molecular characterization of a xylanase from chicken cecum metagenome. *Int. J. Microbiol.* **2017**, *2017*, 4018398. [CrossRef]
15. Warnecke, F.; Luginbühl, P.; Ivanova, N.; Ghassemian, M.; Richardson, T.H.; Stege, J.T.; Cayouette, M.; McHardy, A.C.; Djordjevic, G.; Aboushadi, N. Metagenomic and functional analysis of hindgut microbiota of a wood-feeding higher termite. *Nature* **2007**, *450*, 560. [CrossRef]
16. Li, R.; Kibblewhite, R.; Orts, W.J.; Lee, C.C. Molecular cloning and characterization of multidomain xylanase from manure library. *World J. Microbiol. Biotechnol.* **2009**, *25*, 2071–2078. [CrossRef]
17. Cai, J.; Chen, X.L.; Fan, J.X.; Huang, X.M.; Li, R.; Sun, X.D.; Li, Q.Q.; Li, D.Y. Cloning and heterologous expression of a novel xylanase gene TAX1 from *Trichoderma atroviride* and its application in the deconstruction of corn stover. *Appl. Biochem. Biotechnol.* **2021**, *193*, 3029–3044. [CrossRef]
18. Li, H.; Wu, H.; Jiang, F.; Wu, J.; Xue, Y.; Gan, L.; Liu, J.; Long, M. Heterologous Expression and Characterization of an Acidic GH11 Family Xylanase from *Hypocrea orientalis*. *Appl. Biochem. Biotechnol.* **2018**, *184*, 228–238. [CrossRef]
19. Li, G.; Zhou, X.; Li, Z.; Liu, Y.; Liu, D.; Miao, Y.; Wan, Q.; Zhang, R. Significantly improving the thermostability of a hyperthermophilic GH10 family xylanase XynAF1 by semi-rational design. *Appl. Microbiol. Biotechnol.* **2021**, *105*, 4561–4576. [CrossRef]
20. Liew, K.J.; Ngooi, C.Y.; Shamsir, M.S.; Sani, R.K.; Chong, C.S.; Goh, K.M. Heterologous expression, purification and biochemical characterization of a new endo-1,4-β-xylanase from Rhodothermaceae bacterium RA. *Protein Expres. Purif.* **2019**, *164*, 105464. [CrossRef]
21. Xu, B.; Dai, L.M.; Li, J.J.; Dent, M.; Miao, H.B.; Zhou, J.P.; Mu, Y.L.; Wu, Q.; Tang, X.H.; Yang, Y.J.; et al. Molecular and Biochemical Characterization of a Novel Xylanase from *Massilia* sp. RBM26 Isolated from the Feces of Rhinopithecus bieti. *J. Microbiol. Biotechnol.* **2015**, *26*, 9–19. [CrossRef] [PubMed]
22. Xiao, Z.Z.; Grosse, S.; Bergeron, H.; Lau, P.C.K. Cloning and characterization of the first GH10 and GH11 xylanases from *Rhizopus oryzae*. *Appl. Microbiol. Biotechnol.* **2014**, *98*, 8211–8222. [CrossRef] [PubMed]
23. Shental-Bechor, D.; Levy, Y. Effect of glycosylation on protein folding. A close look at thermodynamic stabilization. *Proc. Natl. Acad. Sci. USA* **2008**, *105*, 8256–8261. [CrossRef] [PubMed]
24. Fonseca-Maldonado, R.; Vieira, D.S.; Alponti, J.S.; Bonneil, E.; Thibault, P.; Ward, R.J. Engineering the pattern of protein glycosylation modulates the thermostability of a GH11 xylanase. *J. Biol. Chem.* **2013**, *288*, 25522–25534. [CrossRef]

25. Yi, W.; Clark, P.M.; Mason, D.E.; Keenan, M.C.; Hill, C.; Goddard, W.A.; Peters, E.C.; Driggers, E.M.; Hsieh-Wilson, L.C. Phosphofructokinase 1 glycosylation regulates cell growth and metabolism. *Science* **2012**, *337*, 975–980. [CrossRef]
26. Helenius, A.; Aebi, M. Roles of N-linked glycans in the endoplasmic reticulum. *Annu. Rev. Biochem.* **2004**, *73*, 1019–1049. [CrossRef]